ISSN 2347-3487

Stability Investigation in the Optical Properties of Thermally Evaporated $Ge_5Se_{95-x}Zn_x$ Thin Films

Austine A. Mulama[a*], Julius M. Mwabora[b], Andrew O. Oduor[c], Cosmas M. Muiva[d], Boniface Muthoka[e], Betty N. Amukayia[f], Drinold A. Mbete[g]

[a,c]Department of Physics and Materials Science, Maseno University, 333-40105, Maseno, Kenya
[a*]mulamaustine@gmail.com
[c]andrewoduor22@gmail.com
[b,e]Department of Physics, University of Nairobi, 30197-00100, Nairobi, Kenya
[b]mwabora@uonbi.ac.ke
[e]bmuthoka@uonbi.ac.ke
[d]Department of Physics, Botswana International University of Science and Technology, 10071, Palapye, Botswana
[d]muivac@biust.ac.bw
[f]Department of Physics, Chamakanga Girls High School, 157-50302, Chamakanga, Kenya
[f]omina.betty84@gmail.com
[g]Department of Mathematics, Masinde Muliro University of Science & Technology, 190-50100, Kakamega, Kenya
[g]drinoldmbete123@gmail.com

ABSTRACT

Selenium-based chalcogenides are useful in telecommunication devices like infrared optics and threshold switching devices. The investigated system of $Ge_5Se_{95-x}Zn_x$ ($0.0 \leq x \leq 4$ at.%) has been prepared from high purity constituent elements. Thin films from the bulk material were deposited by vacuum thermal evaporation. Optical absorbance measurements have been performed on the as-deposited thin films using transmission spectra. The allowed optical transition was found to be indirect and the corresponding band gap energy determined. The variation of optical band gap energy with the average coordination number has also been investigated based on the chemical bonding between the constituents and the rigidity behaviour of the system's network.

Indexing terms/Keywords

Thermal evaporation; Ge-Se-Zn alloy; optical characterization.

Academic Discipline And Sub-Disciplines

School of Biological and Physical Sciences: Physics

SUBJECT CLASSIFICATION

Condensed Matter Physics-Properties of Thin Films

TYPE (METHOD/APPROACH)

Research article-Experimental

ISSN 2347-3487

1. INTRODUCTION

Chalcogenide glasses possess very low phonon energies useful in infrared optical devices due to their large, heavy atoms and the low frequency of vibration of metal-chalcogen bonds [1, 2]. They are highly transparent from the visible to the mid- infrared wavelengths, have high refractive indices and are optically highly nonlinear. This makes them suitable for ultra-fast switching in telecommunication systems. Their atomic structures are flexible and viscous. They possess band gap energy of about $2eV$, which decreases in the sequence of sulphur, selenium and tellurium, reflecting enhanced metallic character [3]. In addition, they are quite sensitive to the absorption of electromagnetic radiation and as a result, under illumination, they show a variety of photo-induced changes. These glasses can be applied in the formation of different optical instruments, lenses, and in glass fibers based on their properties like dispersion of the refractive index, which is composition dependent [4].

The absence of long-range order in amorphous materials allows the modification of their optical properties to a specific technological application by changing their chemical composition through doping. Hence, the area of chalcogenide glasses or non-oxide glasses especially selenium-based chalcogenides is still growing and open for investigation. The weaknesses associated with pure amorphous selenium (a-Se) glasses such as ageing effect and thermal instability is eliminated with the addition of other elements like lead, antimony, bismuth, which enhances material strength by increasing the cross linking in the glassy network [5, 6]. The future generation devices in telecommunication and related applications will greatly rely on the development of materials which possess optimized physical properties. This calls for research into material choice, stability and long-term ageing behavior. The glassy alloys of the Ge-Se system are widely used for various applications in many fields such as switching, memory elements, optoelectronic devices and in infrared optics [7]. The binary Ge-Se system usually has unstable stability which is improved by doping with elements like lead, bismuth, arsenic, etc. The effect of impurity in amorphous semiconductors may alter the mobility of the charge carriers or may introduce structural changes in the amorphous materials with or without modification of the localized states in the forbidden gap. The Ge-Se-Zn glasses show a memory switching behavior. However, very little studies have been carried out on the Ge-Se-Zn glass system [8]. In fact there is scarcity of literature on the optical properties of the Ge-Se-Zn thin films. The present study is based on Ge-Se glassy system containing Zn as the third substitute. Addition of a third element like Zn creates compositional and configurational disorders in the Ge-Se system which helps tune the optical and thermal properties of the system.

2. EXPERIMENTAL METHODS

2.1. Substrate preparation

Production of high quality amorphous thin films of Ge-Se-Zn alloy with good long-term stability against crystallization requires that the films are deposited onto a substrate with a surface that is clean from oil, dust and other contaminants. If the surface of the substrate is contaminated with foreign substances like oil or grease, the adhesion of film will be degraded and there will be a tendency for the thin film to crack and peel. Amorphous selenium is unstable and tends to crystallize quickly in the presence of contaminants. Humidity and oil from human fingertips usually accelerate the crystallization process. The standard glass substrates were cleaned in a mixture of deionised water, liquid detergent and sodium hydroxide. Powersonic 405 Ultrasonic cleaner with three quarters full of deionised water was used to rinse the glass slides for 40 minutes at 45℃ to ensure complete removal of dirt. The cleaned glass slides were sprayed with pressurised argon gas to remove deionised water. The glass slides were used for coating immediately after the cleaning exercise to avoid contamination with the environment. Latex gloves were worn during cleaning of the glass slides to prevent the skin oils from contaminating the slides.

2.2. Sample preparation and deposition

Bulk samples of $Ge_5Se_{95-x}Zn_x$ (x = 0.0, 1.5, 2.0, 3.5, and 4.0 at. %) were prepared by melt quenching technique. Selenium, germanium, and zinc (99.999% pure) were weighed according to their atomic percentages in powder form on electronic balance (LIBROR, AEG-120; Japan). The weighed samples were sealed in quartz ampoules (length ~ 10cm, internal diameter ~ 0.8cm) evacuated to 5.3×10^{-5}mbar. The sealed ampoules were kept in a programmable furnace where the temperature was raised from 26℃ to 800^{o}C gradually at a rate of 4^{o}C per minute and maintained at this temperature for 24 hours with rocking after every 45 minutes to avoid phase separation [9]. Gradual increase in temperature helps avoid explosions that can occur. The ampoules were quenched by removing them from the furnace (at 800^{o}C) and dropping in ice cold water. Quenching ensured that the different atoms were randomly mixed to form continuous homogeneous non-crystalline films on cleaned glass substrates. The ampoules were broken to obtain the solid alloy that was crushed into powder for thermal evaporation. The method is flexible and easy to use. The deposition chamber pressure was 4.1×10^{-5}mbar and the deposition rate was 25Ås^{-1} (Edwards Auto 306 Vacuum System, UK). The coating was performed at room temperature.

2.3. Transmittance, reflectance, film thickness, and X-Ray diffraction measurements

Transmittance and reflectance were measured on a SolidSpec. 3700 Deep Ultra-Violet (DUV) spectrophotometer (SolidSpec. 3700, DUV, UK) at normal incidence. The transmittance and reflectance data were used for the calculation of optical constants such as optical band gap, refractive index, extinction coefficient, and absorption coefficient. Film thickness was determined using a computerized KLA-Tencor Alpha-Step IQ surface profiler. The X-Ray diffraction

ISSN 2347-3487

patterns were made on Philips, PW1710, diffractometer, UK. The incident radiation source was CuK_α (λ = 1.5406Å). The 2θ range was 5^o-60^o, with a step size of 0.025^o. The generator settings were 35mA and 40kV. The measurements were done at room temperature.

2.4. Calculation of optical constants

Transmission spectra based on maximum transmission (T_M) and minimum transmission (T_m) were used to calculate the refractive index (n) under Swanepoel's envelope method [10],

$$n = [M + (M^2 - n_g^2)^{1/2}]^{1/2} \quad (2.1)$$

where $M = \frac{2n_g}{T_M} - \frac{(n_g^2+1)}{2}$ for transparent region, $M = 2n_g \frac{(T_M - T_m)}{T_M T_m} + \frac{(n_g^2+1)}{2}$ for weak and medium absorption, and n_g is the refractive index of the glass substrate.

The extinction coefficient (k) can be calculated from the following relation [11],

$$k = \frac{\alpha\lambda}{4\pi} \quad (2.2)$$

where λ is the wavelength and α is the absorption coefficient as given in equation (2.3),

$$\alpha = d^{-1} \ln T^{-1} \quad (2.3)$$

In equation (2.3), d is the film thickness which can be calculated if refractive indices n_1 and n_2 at two adjacent maxima or minima corresponding to their wavelengths λ_1 and λ_2 are known. This film thickness is given by [12],

$$d = \frac{\lambda_1\lambda_2}{2(\lambda_1 n_2 - \lambda_2 n_1)} \quad (2.4)$$

The optical conductivity (σ) depends on the absorption coefficient (α) [11],

$$\sigma = \frac{\alpha n c}{4\pi} \quad (2.5)$$

where n is the refractive index of the as-deposited thin films and c is the speed of light.

The real part (ε') and imaginary part (ε'') of the dielectric constant are determined from the relation [13],

$$\varepsilon' = n^2 - k^2 \quad (2.6a)$$

and

$$\varepsilon'' = 2nk \quad (2.6b)$$

To obtain the optical band gap energy in the high absorption region $(\alpha \geq 10^4 cm^{-1})$ of the as-deposited thin films, the absorption spectrum followed the Tauc's relation [14],

$$(\alpha h\nu)^{1/2} = (h\nu - E_g) \quad (2.7)$$

where $h\nu$ is the photon energy and E_g is the optical band gap energy.

The average coordination number for ternary selenium system like $Ge_5Se_{95-x}Zn_x$ (x = 0.0, 1.5, 2.0, 3.5, and 4.0 at. %) under investigation, can be obtained from the following expression [15];

$$\xi = 2(x+1) \quad (2.8)$$

where x is the atomic percentage.

3.0 RESULTS AND DISCUSSIONS

3.1 Film thickness and nature of deposited thin films

Measured film thickness on a surface profiler was 200±10nm. The calculated thickness based on Swanepoel method was within ±5nm accuracy compared with the thickness obtained from the surface profiler. The as-deposited thin films were amorphous due to absence of pronounced peaks (Fig. 1). The observed humps is the effect of the glass substrate.

ISSN 2347-3487

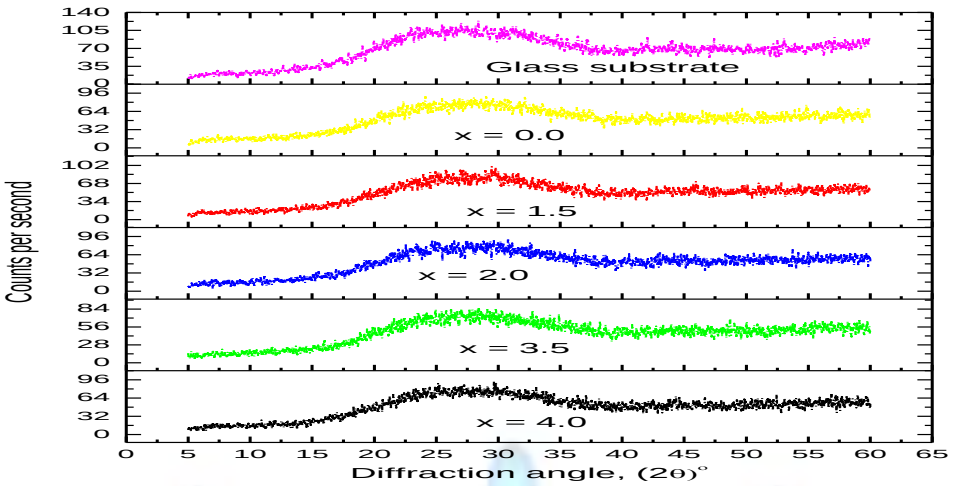

Figure 1: XRD patterns of as-deposited thin films

3.2 Transmittance and reflectance

Figure 2 shows the transmittance (%) and reflectance (%) against wavelength (nm) of the as-deposited thin films.

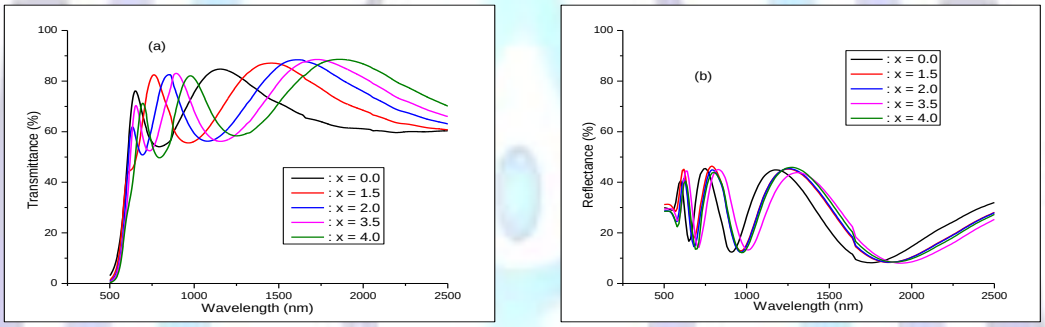

Figure 2: (a) Transmittance (%) and (b) reflectance (%) against wavelength (nm)

The transmittance and reflectance spectra are characterized by interference patterns between 600nm-2000nm, an indication of thickness uniformity of the as-deposited thin films. The observed fringes were used in the calculation of the refractive indices according to Swanepoel method (Eq. 2.1) [10]. The transmission spectra in Fig. 2(a) exhibits transmittance shift towards the higher wavelength as zinc concentration increases from 0 at. % to 4 at. % especially in visible region. This can be an indication of photosensitive as-deposited thin films. There is observed decrease in transmittance with addition of zinc content in the visible region (Fig. 2a). This could be due to absorption of light by the as-deposited thin films [16].

3.3 Refractive index, extinction and absorption coefficients, and optical conductivity.

Refractive index, extinction coefficient and absorption coefficient against wavelength are shown in Figure 3. The variation of refractive index with wavelength for $Ge_5Se_{95-x}Zn_x$ (x = 0.0, 1.5, 2.0, 3.5, and 4.0 at. %) thin films is presented in Fig. 3(a). It indicates a decrease in refractive index with increase in wavelength. This could be attributed to the strong effects of surface and volume imperfections in chalcogenide glasses. It also indicates the normal dispersion in thin films. The oscillatory behaviour in the extinction and absorption coefficients noticed in Figs. 3(b) & 3(c) is the effect of reflection in the as-deposited thin films . The values of extinction coefficient increases with increase in photon energy or decreases with increase in photon wavelength. This may be in view of the large absorption coefficient ($\geq 10^4 cm^{-1}$) for higher energy values or lower wavelength. The optical conductivity directly depends on the absorption coefficient and is found from Fig. 3(d) to increase sharply for higher energy values or decrease with wavelength owing to large absorption for the as-deposited thin films [17].

ISSN 2347-3487

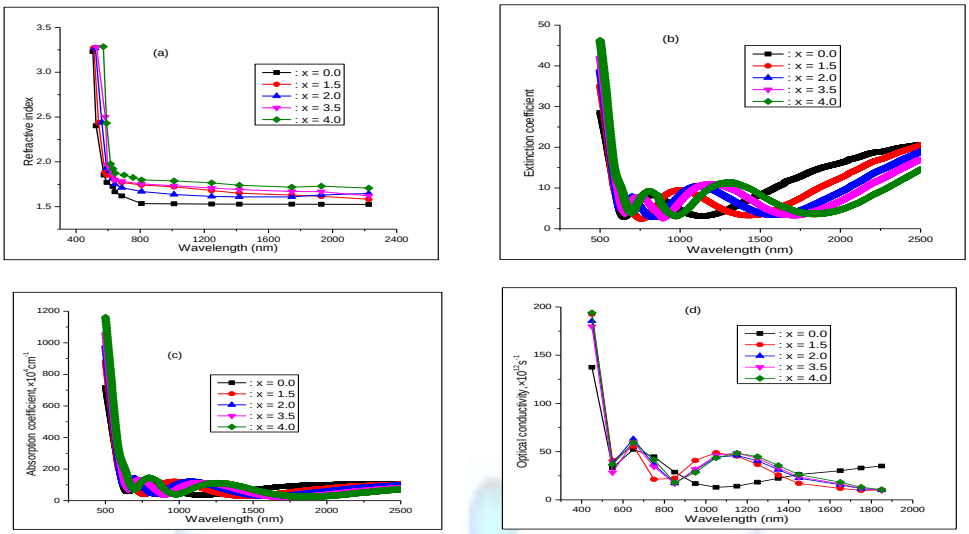

Figure 3: (a) Refractive index, (b) Extinction coefficient, (c) Absorption coefficient (cm^{-1}), and (d) Optical conductivity (s^{-1}) against wavelength (nm)

3.4 Optical band gap energy

A plot of $(\alpha hv)^{1/2}$ $(eVcm^{-1})^{1/2}$ against photon energy (eV) is given in Fig. 4. The spectrum shows a square-root dependence.

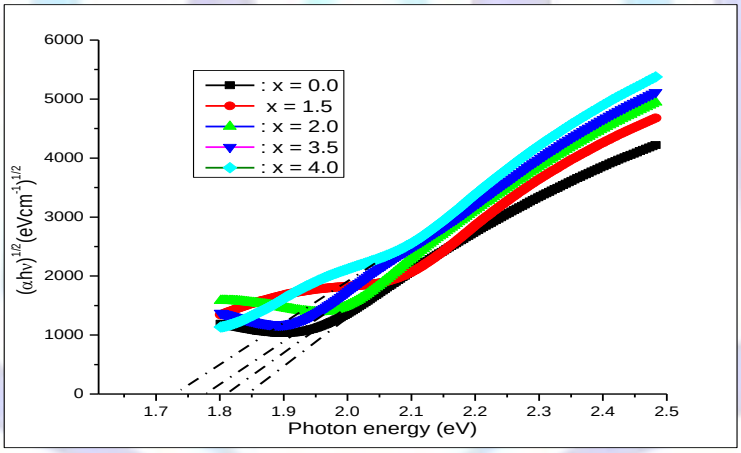

Figure 4: $(\alpha hv)^{1/2}$ $(eVcm^{-1})^{1/2}$ against photon energy (eV)

The optical band gap was determined by the intercept of the extrapolations to zero with the photon energy axis: $(\alpha h\nu)^{1/2} \rightarrow 0$ as shown in Fig. 4 called Tauc extrapolation [14].

3.5 Effect of Zinc content and substrate temperature on the optical parameters of the as deposited thin films

3.5.1 Refractive index, extinction coefficient, real and imaginary parts of dielectric constant.

Figure 5 show the refractive index (a), extinction coefficient (b), real (c) and imaginary (d) parts of dielectric constant against zinc concentration at different substrate temperatures. It is noted that the refractive index increases with increase in zinc content (Fig. 5a). This could be as a result of polarizability, increased density, rigidity, and compactness of the as-deposited Ge-Se-Zn network due to zinc addition. The increase of refractive index with increase in impurity concentration agrees with other previous studies [6, 11, 13]. Increase in refractive index with increase in zinc concentration can be explained in terms of narrowing of pores in the deposited thin films. This is because the film surface gets denser as the impurities of zinc increase. A denser material has a larger refractive index than a less dense material since more electric dipoles are activated when the material is exposed to electric field of the incoming light radiation [11]. The refractive index is also observed to increase with increase in substrate temperature. The absorption coefficient (Fig.5c) has been demonstrated to increase with both increase in zinc content and substrate temperature, an indication of well adhered and compact thin films at higher substrate temperature. The behaviour demonstrated by Fig.5(c) and Fig.5(d) is related to

ISSN 2347-3487

Fig.5(a) and Fig.5(b) respectively due to the corresponding relationships among the optical constants under consideration. The real part of the dielectric constant shows how much it will slow down the speed of light in the material under investigation, whereas the imaginary part shows how a dielectric material absorbs energy from an electric field due to dipole motion. The knowledge of the real and the imaginary parts of the dielectric constant provides information about the loss factor which is the ratio of the imaginary part to the real part of the dielectric constant [13]. The real part of the dielectric constant represents the in-phase component of the dielectric response function and results in dispersion. This physically means refraction of the electromagnetic radiation as it passes through the deposited films.

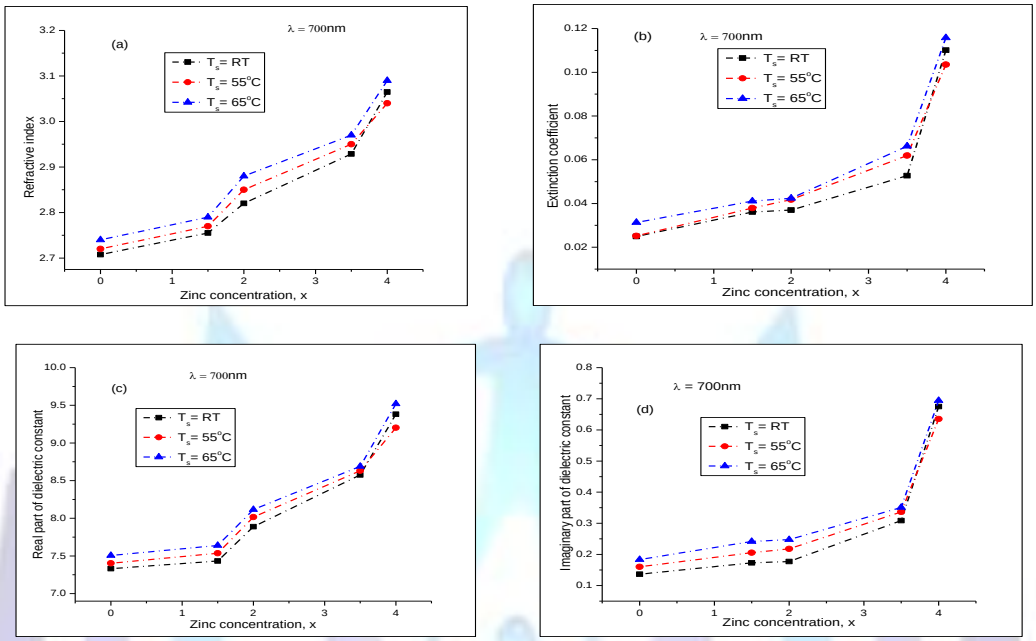

Figure 5: (a) Refractive index, (b) Extinction coefficient, (c) Real part, and (d) Imaginary part of dielectric constant against Zinc concentration.

3.5.2 Absorption coefficient, energy band gap, and optical conductivity

Absorption coefficient (cm^{-1}), band gap energy (eV), and optical conductivity (s^{-1}) against zinc concentration at various substrate temperatures is presented in figure 6.

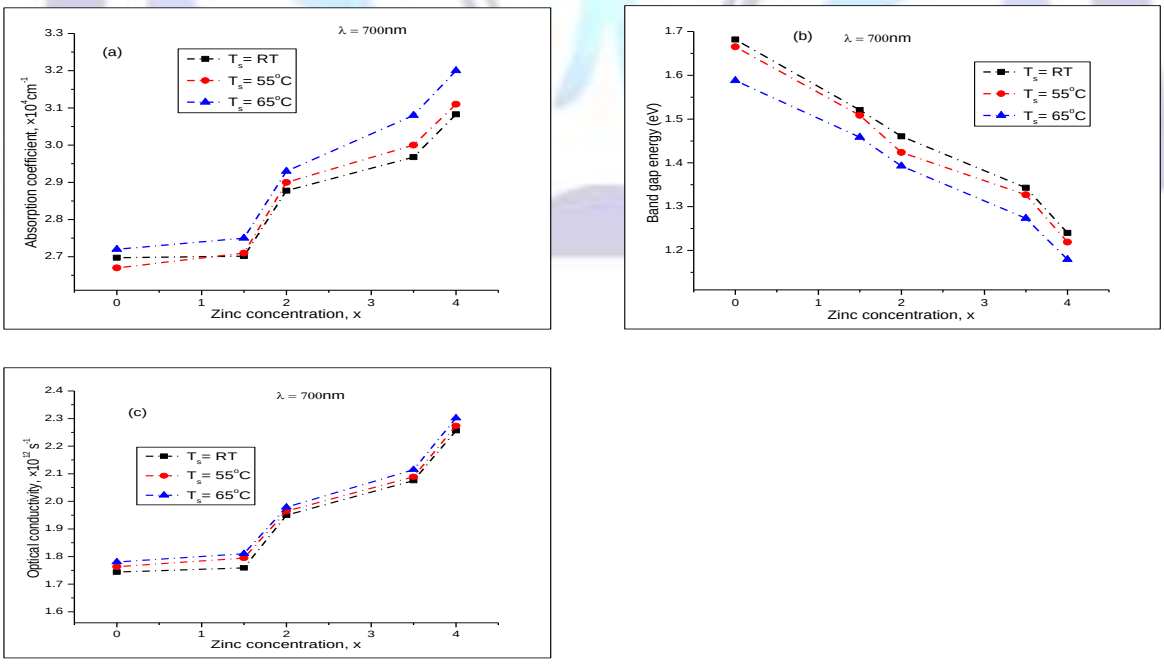

Figure 6: (a) Absorption coefficient (cm^{-1}), (b) Band gap energy (eV), and (c) Optical conductivity (s^{-1}) against Zinc concentration.

ISSN 2347-3487

It is noted from Fig. 6(a), that the absorption coefficient increases with increase in zinc addition at various substrate temperature. A remarkable rise in absorption coefficient has been observed at 2 at. % of zinc. This could be the result of chemical disorder in chalcogenide glasses. This disorder produces large charge in the local potential through the coulombian interaction because of the large ionic contribution to the bonding in chalcogenide glasses [18]. Since the optical conductivity depends on the absorption coefficient, Fig.6(c) shows a direct correspondence. Optical band gap energy is observed to decrease with increase in zinc content (Fig.6b). This may be ascribed to the presence of localized states in the forbidden gap according to [19]. Addition of zinc increases the concentration of localized states leading to lowering the optical band gap. The decrease in the optical band gap can also be as a result of decrease in the average bond energy of the system according to [20], since optical band gap is bond sensitive property.

3.6 Band gap energy and average coordination number

A plot of band gap energy (eV) against average coordination number is given in Fig.7. A close examination of Fig.7 indicates an increase in band gap energy with increase in average coordination number. The values of the average coordination number for the investigated compositions range between 2.0 and 2.2. As can be noted from Fig.7, the optical band gap energy-average coordination number dependence exhibits a minimum at average coordination number of 2.0. The observed trend may be an indication of a change from an under-cross linked to a constrained network in the as-deposited thin films. The increase in the average coordination number to 2.2 can lead to increased interaction between the atomic species under investigation [21]. Low average coordination number makes the properties of the system under study to be very sensitive to the weak Van der Waal's forces. As the coordination number increases beyond 2.0, covalent bonds come into play and this increases the viscosity of the system due to the stressed rigidity.

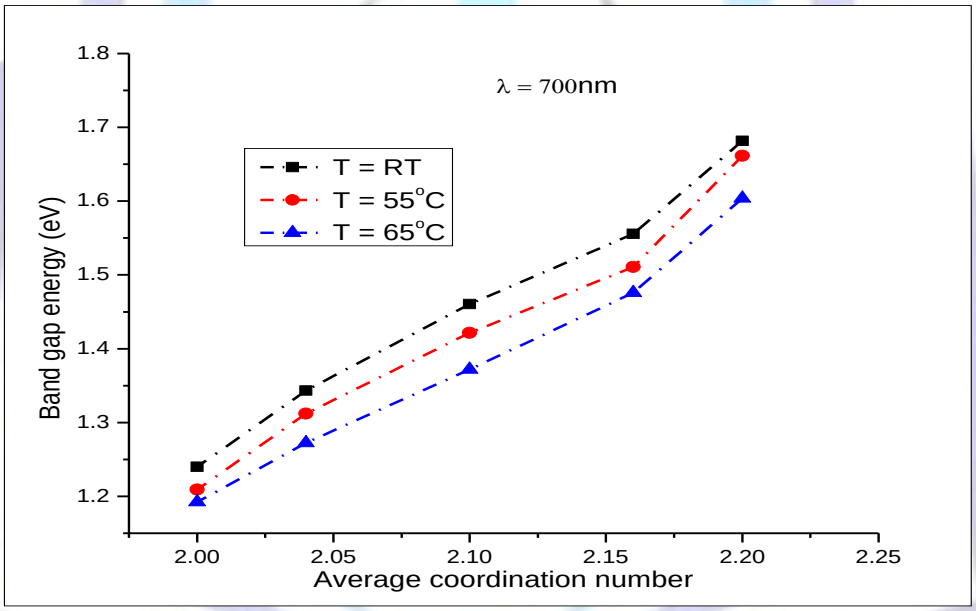

Figure 7: Band gap energy (eV) against average coordination number.

4.0 CONCLUSION

The study considered $Ge_5Se_{95-x}Zn_x$ ($0.0 \leq x \leq 4$ at.%) system. Addition of zinc as a third element helps in cross linking the system making the system to be more stable and rigid. As a result, there is improved optical properties of the as-deposited Ge-Se-Zn thin films. The thin films produced were amorphous, homogeneous, and uniform. This has been shown by absence of prominent peaks in the X-Ray diffraction patterns and the oscillatory nature of both transmittance and reflectance spectra.

ACKNOWLEDGMENTS

The authors wish to thank Ms. Everlyne Odera (University of Nairobi) and Mr. Edward Atito (Maseno University) for their technological advice and in experimental set ups.

ISSN 2347-3487

REFERENCES

[1] Borisova, Z. U. 1981. Glassy semiconductors, 7th Edition. Plenum Press, New York.

[2] Schardt, R. C. 2000. Photodarkening of germanium-selenium glasses induced by below-band gap light. Ph.D dissertation, University of Florida, U.S.A, 28-179

[3] Zallen, R. 1983. The physics of amorphous solids. John Wiley & Sons, NEW York.

[4] Kumar, K., Sharma, P., Katyal, S. C., and Thakur, N. 2011. Optical parameters of ternary $Te_{15}(Se_{100-x}Bi_{x)85}$ thin films deposited by thermal evaporation. Phys. Scr. 84(045703), 1-6

[5] Majeed Khan, M. A., Zulfequar, M., and Husain, M. 2003. Optical investigation of a-$Se_{100-x}Bi_x$ alloys. Optical Materials, 22, 21-29

[6] Mulama, A. A., Mwabora, J. M., Oduor, A. O., and Muiva, C. M. 2014. Optical properties and Raman studies of amorphous Se-Bi thin films. The African Review of Physics, 9(6), 33-37.

[7] Sharma, I. and Barman, P. B. 2010. Non-linear refractive index of a-Ge-Se-In-Bi glassy thin films. Advances in Applied Science Research, 1(1), 189-196

[8] Junaghadwala, S. 2011. Metal-modified Ge-Se glass films and their potential for nanodipole junctionless photovoltaics. Ph.D dissertation, University of Toledo, 38-45

[9] Popescu, M. 2006. Self –organization in amorphous semiconductors and chalcogenide glasses. Journal of Advanced Materials, 8(6), 2164-2168

[10] Swanepoel, R. 1983. Determination of the thickness and optical constants of amorphous silicon. Journal of Physics E: Science Intrum. 16, 1214-1218

[11] Guenther, R. D. 2000. Modern optics. John Wiley & Sons, Singapore.

[12] Pandey, V., Tripathi, S. K., and Kumar, A. 2006. Optical properties of Sb_xSe_{1-x} thin films. Physica B. 229, 249-251.

[13] Goswami, A. 1997. Thin film fundamentals. New Age International Publishers, New Delhi, India.

[14] Tauc, J. 1974. Amorphous and liquid semiconductors. Plenum Press, London & New York.

[15] Sreeram, A. N., Varshneya, A. K., and Swiler, D. R. 1991. Molar volume and elastic properties of multicomponent chalcogenide glasses. Journal of Non-Crystalline Solids, 128, 294-309.

[16] Mulama, A. A., Mwabora, J. M, Oduor, A. O., Muiva, C. M., and Walloga, C. M. 2014. Effect of Ga incorporation and film thickness on the optical properties of as-deposited amorphous Ga_xSe_{1-x} thin films. IOSR Journal of Applied Physics, 6(5), 1-6.

[17] Sharma, P., Sharma, V., and Katyal, S. C. 2006. Variation of optical constants in $Ge_{10}Se_{60}Te_{30}$ thin films. Chalcogenide Letters, 3(10), 73-79.

[18] Connnell, G. A. N. 1985. Optical properties of amorphous semiconductors. Springer Berlin, Heidelberg.

[19] Davis, E. A. and Mott, N. F. 1979. Electronic processes in non-crystalline materials, 2nd Edition, Clarendon Press, Oxford.

[20] Bicerano, J. and Ovshinsky, S. R. 1985. Chemical bond approach to the structures of chalcogenide glasses with reversible switching properties. Journal of Non-Crystalline Solids, 74(1), 75-84.

[21] Schottmiller, J., Tabak, M., Lucovsky, G., and Ward, A. 1970. The effect of valency on transport properties of in vitreous binary alloys of selenium. Journal of non-Crystalline Solids, 4, 80-96.